ELSEVIER

Photosystem II of green plants. Oxidation and deprotonation of the same component (histidine?) on $S_1^* \Rightarrow S_2^*$ in chloride-depleted centers as on $S_2 \Rightarrow S_3$ in controls

Michael Haumann, Wolfgang Drevenstedt, Monika Hundelt, Wolfgang Junge *

Abt. Biophysik, Fachbereich Biologie / Chemie, Universität Osnabrück, 49069 Osnabrück, Germany

Abstract

The oxygen-evolving complex (OEC) of green plants accumulates four oxidizing equivalents to produce molecular oxygen from water. At least two equivalents are stored on the catalytic tetra-manganese cluster. How many and which steps oxidize an amino acid residue instead is under debate. We studied the progression towards higher oxidation states in dark-adapted, chloride-depleted Photosystem II core particles and thylakoids from pea, and monitored from nano- to milliseconds absorption transients from the near-UV into the near-IR spectral regions that directly or by electrochromism reflect the oxidation/reduction of the primary (P_{680}), secondary (Y_Z) and tertiary electron donors (Mn_4, histidine?). When starting from the first oxidation state and with the cofactor Cl^- removed, we found that the OEC stored only two oxidizing equivalents if the cofactor Cl^- had been removed. The first equivalent was passed via Y_Z to an as yet chemically ill-defined component, X, that resembled histidine according to its UV/ VIS difference spectrum. The second equivalent was stored on Y_Z itself. Based on a spectral analysis we propose that the same component X (His?) stores the oxidizing equivalent during the second transition, $S_2 \Rightarrow S_3$, in unperturbed material. Our measurements at high time resolution of the concomitant proteolytic reactions led us to propose that during the transition $X^{red} \rightarrow X^{ox}$ a proton is ejected into the aqueous phase. We interpret these data in terms of an electrostatic control by Cl^- of the midpoint potential of Mn_4 relative to X (His?) and Y_Z.

1. Introduction

Photosystem II (PS II) of cyanobacteria and green plants is unique among photosynthetic reaction centers in using water as terminal electron donor. The electropositive side of PS II is connected to the oxygen evolving complex (OEC) which incorporates a tetra-nuclear manganese clus-

ter that faces the lumenal side of the thylakoid membrane. The sequential absorption of four quanta of light leads to the abstraction of four electrons from the OEC, that are sequentially transferred from the primary donor P_{680} to the two quinone acceptors at the other side of the membrane. During each step P_{680}^+ is reduced via tyrosine-161 on subunit D1 (Y_Z) by the OEC. The five increasingly oxidized states of the OEC are named S_0 to S_4. S_4 decays spontaneously into S_0 under release of dioxygen. Usually, S_1 is most stable in the dark (for recent reviews see [1–3]).

It is mechanistically important but still under debate whether all positive charges are transiently accumulated only on manganese or also on amino acid cofactors [4–7]. Detailed schemes which involve redox reactions of certain amino acids, in particular histidine, have been hypothesized [8,9]. It is generally accepted that transition $S_1 \Rightarrow S_2$ represents the oxidation of manganese, whereas $S_2 \Rightarrow S_3$ might involve another component. The EPR multiline signal appearing when state S_2 is formed is attributable to the

---

formation of a mixed valence state of the Mn-cluster [10]. This is compatible with an upshift of the manganese K-edge by about 1 eV associated with transition $S_1 \Rightarrow S_2$ [11] contrasting to a smaller shift on $S_2 \Rightarrow S_3$ [11]. The latter is no longer under contention (compare [12], T. Ono, personal communication at the 10th Photosynthesis Congress, 1995, Montpellier). The picture emerging from UV difference spectra is less clear. The more recently published difference spectra of $S_1 \Rightarrow S_2$ differ from the one of $S_2 \Rightarrow S_3$ [13,14], whereas they are similar in the older literature [15]. The increase from step to step of the transfer time of electrons to Y_Z^{ox} [16,17] has been explained (if present, see [18]) by the electrostatic effect of charge accumulation in the OEC. These data do not, however, prove the stepwise accumulation of charges on Mn. Oscillations of the rate of the reduction of P_{680}^+ [19] and, more or less in parallel, of the extent of stable local electrochromic bandshifts in the blue and red spectral regions [20,21] have also been attributed to charge accumulation in the OEC ([22]; see [23] for review). In this case, the oscillations were tentatively attributed to the electrostatic balance between electron abstraction and proton release. The absence of proton release on transition $S_1 \Rightarrow S_2$ [24] was thought to result in an additional positive charge in S_2 [22]. We have recently shown that the electrostatic situation in the OEC is almost independent of the observed extent of proton release [17]. To account for the rather invariant pattern of local electrochromism (0:1:0: $-$ 1, starting from $S_0 \Rightarrow S_1$) under variation of the pattern of proton release we proposed that the pronounced oscillations may result from the deposition of charges (electron holes and protons) at different positions in the OEC [23].

Work with modified PS II provides more direct evidence for the involvement of another amino acid. In the absence of the essential ionic cofactors chloride or calcium, oxygen evolution is inhibited [25,26], although the OEC can still store two oxidizing equivalents when dark-adapted material is excited by flashing light [27,28]. From the third flash on a rapid charge recombination between Q_A^- and P_{680}^+ occurs in about 150 μs [28–30]. EPR and UV studies on calcium-depleted centers gave evidence for the oxidation of an amino acid residue other than Y_Z on the second transition, presumably histidine [31,32]. Based on thermoluminescence data the oxidation of histidine has also been proposed for Mn-depleted material [33]. The nature of the first two oxidation steps in chloride-depleted material, however, is under debate: Certain EPR data have been interpreted as indicating the oxidation of Mn on the first and the metastable formation of Y_Z^{ox} on the second transition [28,34,35]. Also based on EPR work, the oxidation of histidine has been proposed for the first and of Mn for the second transition [29,36,37]. These studies, however, gave no evidence for the functioning of histidine in oxygen evolving centers [38,39]. One interpretation of our earlier work with Cl$^-$-depleted thylakoids was the oxidation of Mn on the first and of histidine on the second

transition [30]. Hence, it is unresolved which components (Mn, Y_Z or His) are oxidized during the first two transitions in Cl$^-$-depleted centers.

In this work we used PS II core particles and thylakoids to compare the effects of charge storage in the OEC in the absence and presence of chloride. Special care was taken to achieve high reversibility of chloride depletion. We investigated flash-induced absorption transients in the near UV (attributable to Mn, Y_Z and perhaps other amino acids), the nanosecond reduction of P_{680}^+ in the near-IR, proton release and electrochromism in the blue and red spectral regions. Our data led us to propose the following sequence of events as caused by two flashes of light: $\check{S}_1 XY_Z \Rightarrow \check{S}_2 XY_Z \Rightarrow \check{S}_2 X^{ox} Y_Z$ in controls and $\check{S}_1 XY_Z \Rightarrow \check{S}_1 X^{ox} Y_Z \Rightarrow \check{S}_1 X^{ox} Y_Z^{ox}$ in Cl$^-$-depleted material (note that we denote by $\check{S}_i$ the ith oxidized state of Mn$_4$ itself). This behaviour can be rationalized by the electrostatic effect of Cl$^-$ on the midpoint potential of the manganese cluster. The difference spectrum of $X^{red} \rightarrow X^{ox}$ resembled the one between histidine and its oxidized OH adduct in vitro [73].

2. Materials and methods

All preparations were based on 12-day-old pea seedlings. *PS II core particles* were prepared according to Ghanotakis [40] modified as in [41]. They were stored at $-80°C$ in 10 mM $CaCl_2$, 5 mM Mes (pH 6.0) and 400 mM sucrose until use.

Chloride depletion of core particles was performed as follows. The stock of core particles was thawed and suspended at 10 μM of chlorophyll in a medium with only 2 mM Mes (pH 6.5). The particles were pelleted by centrifugation at $30000 \times g$ at 4°C and resuspended at about 1 mM of chlorophyll in 2 mM Mes (pH 6.5) and 5 mM $CaSO_4$. For *chloride repletion* the particles were suspended in 5 mM $CaCl_2$ instead of $CaSO_4$ after the centrifugation step. Before the measurements, core particles were resuspended in a medium with either 5 mM $CaSO_4$ or $CaCl_2$ plus 2 mM Mes (pH 6.5) (no Mes in pH measurements). 3.3 μM DCBQ plus 6.6 μM hexacyanoferrate(III) per μM chlorophyll were used as electron acceptors. The rate of oxygen evolution under continuous illumination in Cl$^-$-depleted particles was about 10% of a given control ($\sim$ 1000–1300 μmol O_2/mg Chl per h, similar figures have been reported in the original preparation protocol [40]). It was restored to 100–120% of the control by Cl$^-$ repletion.

Manganese depletion was achieved by washing core particles at 10 μM of chlorophyll in 0.8 M Tris (pH 8.5) plus 5 mM $CaCl_2$ [42]. The pH was readjusted to 6.5 prior to the measurements. Oxygen evolution was less than 10% of the control after this treatment.

Thylakoids were prepared according to [43] with Na_2SO_4 in all media instead of NaCl and frozen at $-80°C$

in 10 mM Na_2SO_4 and 400 mM sucrose until use. For the measurements they were thawed and suspended at 10 μM of chlorophyll in either 10 mM Na_2SO_4 (Cl^--depleted) or 20 mM NaCl (Cl^--repleted) and incubated for 15 min on ice. They were collected by centrifugation (20 000 × g, 4°C) and resuspended at 30 μM of chlorophyll in 10 mM Na_2SO_4 or 20 mM NaCl and 2.6 g/l BSA, 15 μM DNP-INT and 2 mM hexacyanoferrate(III) as electron acceptor. The rates of oxygen evolution in control and Cl^--depleted thylakoids were about 150 and 40 μmol O_2/mg Chl per h. *The washing procedures* were carried out in total darkness.

Oxygen evolution was measured under continuous white light illumination with a Clark-type electrode at 5 μM of chlorophyll (20°C) with 10 mM Mes at pH 6.5. 150 μM DCBQ plus 600 μM hexacyanoferrate(III) were used as electron acceptors.

The chlorophyll to reaction center ratio of core particles was determined by the extent of flash-induced absorption transients at 320 nm under repetitive excitation (10 Hz) as described previously [17]. We found a figure of about 120 chlorophylls per PS II. This figure was somewhat higher than originally reported for this type of preparation [40]. The reason may be the use of pea seedlings as starting material in our case instead of spinach as in [40].

Flash-spectrophotometric measurements were performed with the setup described in [44]. An Nd:YAG laser (532 nm, fwhm 6 ns), a Q-switched Ruby laser (694 nm, FWHM 50 ns), and a xenon flashlamp (Schott RG610 or BG39 + WB 560, fwhm 10 μs) were used as excitation sources. Dark-adapted samples were excited by a train of nine flashes at 100 ms interval. To minimize double hits, either all flashes were given by the Nd:YAG laser or the first flash was given by the Ruby laser and the following ones by the Xenon lamp. With dark-adapted material, every train was recorded with a fresh sample which was filled automatically into the cuvette from a light-shielded reservoir. Dark-adapted samples were totally shielded from light after thawing and kept in darkness for additional 5 min after dilution prior to the measurements. Transients were digitized on a Nicolet Pro92 or a Tectronics DSA602 recorder and stored on a MicroVax computer. Up to 1000 transients were averaged to improve the signal-to-noise ratio. The chlorophyll concentrations were as specified in the Legends to Figures. The optical pathlength was 1 cm.

UV transients which were flash induced at 295 nm were time-resolved to monitor electron transfer from the OEC to Y_Z^{ox} [16]. Electron transfer from P_{680} to Q_A, and away from Q_A^- was measured at 320 nm. 50 μM DCBQ were used as electron acceptor.

Local electrochromism was time resolved at 424 and 443 nm. The transients at 443 nm are composite of transients caused by the oxidation/reduction of P_{680}, Q_A, Y_Z and Mn. The transients at 424 nm are due mainly to Q_A. The difference of the former minus the latter transients resulted in transients which were mainly due to the elec-

trochromism in response to oxidation/reduction of Y_Z and Mn (see [18]).

Difference spectra of absorption transients of the OEC were recorded in a wavelength range from 290 to 450 and 630 to 720 nm as follows. Dark-adapted core particles were excited in the presence of 50 μM DCBQ plus 1 mM hexacyanoferrate(III). Under these conditions Q_A^- and $DCBQ^-$ which are formed by each flash decay in less than 5 ms (here not documented but see [45]). Thus, we sampled the difference of absorption before and 50 ms after each flash. It was practically due to donor side events. The spectrum attributable to Q_A reduction was obtained as the difference before and at 5 ms after a flash in the presence of 25 μM DCBQ as electron acceptor under repetitive excitation. This difference was attributable to $Q_A \rightarrow Q_A^-$ because the transients caused by donor side events were cancelled out due to equal contributions of all S-transitions.

Proton release was recorded in core particles as absorption transients of the pH-indicating dye bromocresol purple (10 μM) at 575 nm as previously [46]. The flash spacing was longer, namely 250 ms, to allow for almost complete relaxation of the pH transients. The time resolution was 1 ms per address. The suspending medium contained no added buffer. With thylakoids proton release was recorded with the membrane adsorbed dye Neutral red (30 μM) as previously [47].

The oxidation / reduction of P_{680} was recorded at 820 nm in either of two ways. (i) Transients were recorded at low time resolution (10 μs per address, electrical bandwidth 100 kHz) by using a xenon flash in the above standard setup. (ii) For high time resolution (2 ns per address) a Nd:YAG laser was used as excitation source. A thermostatted cw laser diode (30 mW, 820 nm) served as measuring light source. The beam of low divergence was directed through a 5 cm long cuvette. Absorption transients were detected by a fast avalanche photodiode. Bursts of fluorescence were suppressed by spatial filtering (distance between cuvette and photodiode about 1 m). Flash burst artifacts were rejected by a super notch filter (532 nm). The electrical dc bandwidth of the system was 150 MHz.

The time course of absorption transients was analyzed in terms of single or double exponentials using commercial routines (Grafit, Erithacus Software).

3. Results

3.1. High reversibility of chloride depletion in PS II core particles

Core particles were prepared and Cl^--depleted in total darkness as described under Materials and Methods. Under continuous illumination the rate of oxygen evolution in Cl^--depleted samples was less than 10% of the one after Cl^--repletion (typically 1000–1300 μmol O_2/mg Chl per

h). The rate in Cl^--depleted material, that served as controls, was sometimes even higher than in samples which were not previously depleted. The restoration was immediate after 5 mM $CaCl_2$ or 10 mM NaCl had been added. The mild washing procedure did not cause any calcium depletion. The half-maximal rate of oxygen evolution was restored with about 2 mM of chloride added as $CaCl_2$ (data not shown) in agreement with data obtained with thylakoids (Lübbers, K. (1994) PhD Thesis, University of Osnabrück). The degree of restoration by Cl^- was less the longer the storage time of Cl^--depleted and diluted material. The half-time of the activity loss by storage in total darkness was about 30 min at room temperature. A chloride containing sample, on the other hand, which was diluted and stored under the same conditions conserved its full activity. To minimize the effect of aging in Cl^--depleted material we chose a time for dilution and storage of the samples of 5 min. As the whole preparation procedure was carried out in total darkness, the core particles were well synchronized, as evident from their behavior under flashing light.

3.2. The nanosecond reduction of P_{680}^+ after the first two flashes of light

It has been reported that only two charges can be stored at the donor side of PS II beyond P_{680} in the absence of chloride [28,29]. However, the rate of reduction of P_{680}^+ has not been resolved in these studies. Fig. 1A shows the oxidation/reduction of P_{680} at low time resolution (10 μs) at 820 nm in dark-adapted, reversibly Cl^--depleted core particles after the first five flashes. Due to the low time resolution, the first two flashes induced smaller transients than the following ones. From the third flash on, larger transients decayed with the following half-decay times and relative extents: 90 μs: 44%, 500 μs: 42% and milliseconds: 14%. A similar set of half-rise-times and relative extents was observed under repetitive excitation at 320 nm (not documented), reflecting the oxidation/ reduction of Q_A^- [48]. This behaviour paralleled the one of the transmembrane charge recombination between P_{680}^+ and Q_A^- in Cl^--depleted thylakoids [30]. With 120 chlorophylls per reaction center (see Materials and Methods and [17]) we calculated an extinction coefficient at 820 nm on the fifth flash of $\Delta\epsilon = 6000\ M^{-1}\ cm^{-1}$. This figure was about 15% smaller than the previously published one for P_{680}^+ of 7000 [49]. We conclude that in our samples about 85% of P_{680}^+ were reduced in micro- to milliseconds on the fifth flash, the rest decayed faster (see next paragraph).

Fig. 1B shows the transients at 820 nm after flashes 1, 2 and 5 now time-resolved at 150 MHz upper bandwidth. In Cl^--depleted material (upper traces) and on the first flash the major portion (70%) of P_{680}^+ was reduced with a half-rise-time of 35 ns (smooth line). A minor component of 10% decayed in 5 μs. On the second flash the 35 ns component was only small (15%) and perhaps due to
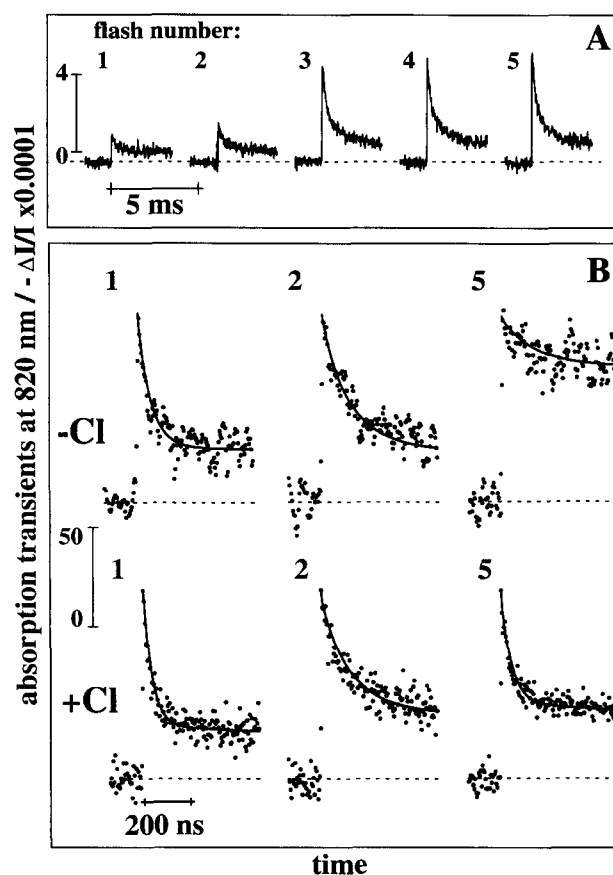

Fig. 1. Absorption transients at 820 nm which indicate the oxidation (upward directed jump) and reduction (decay) of P_{680}^+. (A) Transients induced by the first five flashes in chloride-depleted, dark-adapted core particles. Conditions: 5 μM chlorophyll, the time resolution was 10 μs per address, 90 transients were averaged, exciting flashes from a Q-switched ruby laser (No. 1) and a xenon lamp (Nos. 2–5), respectively. (B) Transients induced by flashes 1, 2 and 5 in Cl^--depleted (top) and control (bottom) core particles. Conditions: 15 μM chlorophyll, 2 ns per address, 40 transients averaged, excitation with a Q-switched, frequency-doubled Nd:YAG laser.

centers not hit by the first flash. The major portion (57%) decayed more slowly, with a half-decay time of 100 ns. From the third flash on, the reduction of P_{680}^+ proceeded mainly in microseconds by charge pair recombination as documented in Fig. 1A. The relative amplitude of the minor 100 ns component was only 20% on the fifth flash. In contrast, in the controls (Fig. 1B, lower traces) the reduction of P_{680}^+ was nearly monophasic on the first flash ($t_{1/2} = 15$ ns, 75%). It slowed down on the second flash (major components of 40 ns (41%) and 280 ns (27%) and further on the third flash (60 ns, 45%; 390 ns, 25%). The decay of the transients on the fourth and fifth flash was again accelerated, mainly to 15 ns (see the 5th flash in Fig. 1B). Period of four oscillations of the decay times are known from the literature [19]. The above figures were obtained by fitting the data with three exponentials plus an offset to account for the microsecond components. The half-decay-times and relative extents of the kinetic compo-

Table 1

Half-rise-times and relative extents of nanosecond electron transfer to P_{680}^+ in Cl^--depleted, dark-adapted PSII core particles and in controls. Kinetic components in the μs range are denoted by (*), charge pair recombination in 90/500 μs with Q_A^- is denoted by (c.r.)

Flash No.:	1	2	3
Material:	half-rise-time of P_{680}^+ reduction/relative extent		
Control	15 ns/75%	15 ns/10%	
		40 ns/41%	60 ns/45%
		280 ns/27%	390 ns/25%
	* 25%	* 22%	* 30%
Cl^--depleted	35 ns/70%	35 ns/10%	
		100 ns/57%	100 ns/24%
	5 μs/10%		
	* 20%	* 28%	(c.r.) 76%

nents of the first three flashes are listed in Table 1. Both in the presence and absence of Cl^-, P_{680}^+ reduction was similarly rapid on the first two flashes. Probably the same donor, Y_Z, was involved in both cases.

3.3. Without chloride, the stability of the first and second terminal electron donor differs

We investigated the stability of the first two oxidized species that were formed in the absence of chloride. Core particles were repetitively excited under variation of the time interval between flashes. The transient that was obtained with a flash period of 5 s is shown in Fig. 2A. P_{680}^+ was reduced nearly monophasically with the same half-decay time of 100 ns (line) that was observed on the second flash with dark-adapted material. The 35 ns component that was observed on the first flash was absent (relative extent less than 10%). Thus, the oxidized component formed on the first flash in dark-adapted samples, which was responsible for the slowing of the reduction of P_{680}^+ from 35 to 100 ns, persisted for at least 5 s. The stability of the component oxidized on the second flash was obtained from a plot of the extent of the 100 ns component as function of the time interval between flashes shown in Fig. 2B. This extent indicated the proportion to which the donor to P_{680}^+, e.g., Y_Z^{ox}, was rereduced between flashes. With 50 μM DCBQ and 100 μM hexacyanoferrate(III)) as electron acceptors the overall half rise-time was 400 ms (solid circles). It was shortened to 180 ms (open circles) in the presence of 500 μM DCBQ, 1 mM hexacyanoferrate(III) and 1 mM hexacyanoferrate(II). These chemicals probably served as extrinsic electron donors for Y_Z^{ox} as reported previously [50,51]. According to these results we expected about 20% of Y_Z to be reduced at flash intervals of 100 ms, which explained the small 100 ns component observed on the reduction of P_{680}^+ on the fifth flash (see Fig. 1B).

3.4. Two charges can be stored in reversibly Cl^--depleted centers, but only one in aged material

With Cl^--depleted samples we found that one source of non-reproducibility was aging. In a Cl^--depleted sample which was stored in the dark for 1.5 h at room temperature and excited repetitively every 5 s, P_{680}^+ was reduced slowly in 5 μs (plus a minor component of 100 ns, Fig. 2C). The deceleration was not reversed by the addition of chloride. A microsecond decay of P_{680}^+ is typically observed in centers which have lost manganese (e.g., by Tris washing [42]). On the other hand, in a control sample that was
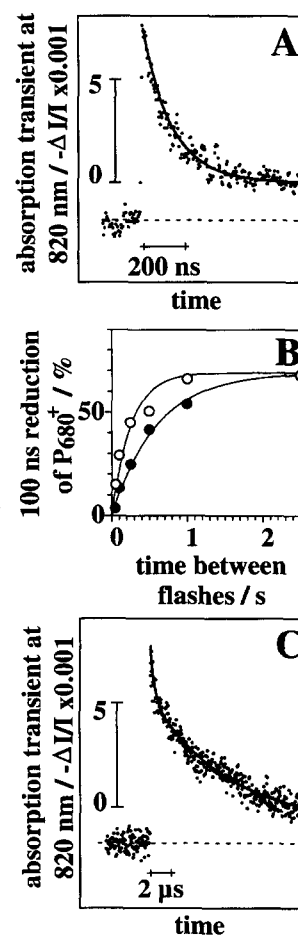

Fig. 2. Oxidation/reduction of P_{680}^+ indicated by absorption transients at 820 nm in core particles. (A) Reversibly Cl^--depleted material. The smooth line was calculated with a half-rise-time of 100 ns and an offset to account for slower components. (B) The 100 ns component of the reduction of P_{680}^+ as function of the time interval between flashes. The data points were determined from measurements similar to the one in (A) with 15 μM chlorophyll. Solid circles: DCBQ 50 μM, hexacyanoferrate(III) 100 μM; open circles: DCBQ 500 μM, hexacyanoferrate(III) and (II) 1 mM. (C) Cl^--depleted material that was aged for 1.5 h. The line was calculated with half-rise times of 100 ns and 5 μs. Note the 5-fold longer x-axis than in (A). Conditions: 15 μM chlorophyll, repetitive Nd:YAG excitation every 5 s in A) and C), digitizing at 2 ns per address (only every 10th point is shown in (C)), 512 transients averaged for each trace.
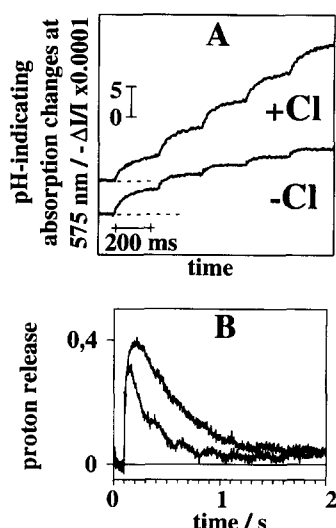
Fig. 3. (A) Proton release after the first five flashes from dark-adapted, Cl^--depleted (bottom) and control (top) PS II core particles (5 μM chlorophyll) with Bromocresol purple (10 μM) at 575 nm. (B) Proton release (ascending) and rebinding measured as in (A) but under repetitive excitation (every 5 s). Upper trace: DCBQ 17 μM, hexacyanoferrate(III) 33 μM; lower trace: DCBQ 170 μM, hexacyanoferrate(III) and (II) 330 μM. 2 ms per address, 10 transients averaged. See text for the respective half-life-times.

incubated for 1.5 h the reduction of P_{680}^+ was still fast (15, 50, 340 ns). Thus, chloride depletion destabilized the OEC, so that irreversible aging was greatly accelerated. Based on the relaxation in microseconds, this destabilisation was probably attributable to the Mn cluster itself.

Dark-adapted, Cl^--depleted samples which were stored in the dark for 30 min revealed a biphasic decay of the transient on the first flash with half-decay times of 5 μs (50%), 35 ns (40%) and in milliseconds. On the second flash given after 100 ms already about 55% of P_{680}^+ were reduced by charge recombination in 90/500 μs, the rest decayed mainly in 100 ns (35%) plus a minor 35 ns contribution (10%). Accordingly, 30 min was about the half-rise-time for the conversion of Cl^--depleted centers into irreversibly damaged ones. In a Tris-washed, dark-adapted sample the transient on the first flash decayed almost monophasically in 5 μs and the one on the second flash nearly completely by charge recombination (data not documented). Accordingly, reversibly Cl^--depleted centers can store two oxidizing equivalents at the donor side whereas irreversibly damaged centers can store only one.

3.5. Cl^- depletion alters the pattern of proton release

Fig. 3A shows proton release as induced by a train of flashes in dark-adapted core particles. In the control (top), the release of slightly less than one proton (0.9) was observed on the first flash and about one proton from then on, as previously found [41]. Without chloride (bottom) the release on flash no. one was slightly greater (1 proton)

than in the control. On the second flash about 0.55 protons were released and much less (0.25) from then on. When only one flash was given to a dark-adapted sample the deprotonation persisted for more than 5 s (data not shown) both in controls and in Cl^--depleted samples. One part of the residual proton release in the latter case, from flash No. 3 on, may be caused by centers which were still active (about 10%), the rest was probably caused by the rereduction of about 20% of Y_Z^{ox} between flashes (due to the relatively wide spacing between flashes, 250 ms). The latter was supported by data in Fig. 3B. The upper trace in Fig. 3B shows proton release when measured under repetitive excitation (period 5 s, compare Section 3.3 in a reversibly Cl^--depleted sample. We observed the initial release of about 0.4 to 0.5 protons which were rebound with a half-rise-time of 450 ms (with 17 μM DCBQ plus 33 μM hexacyanoferrate(III). Under changed electron acceptor conditions, 170 μM DCBQ, 330 μM hexacyanoferrate(III) and 330 μM hexacyanoferrate(II), the rebinding of protons was accelerated to 160 ms (Fig. 3B, lower trace). We attribute the fractional proton release to the formation of Y_Z^{ox} and its reversal to the reduction of Y_Z^{ox} probably by hexacyanoferrate(II) [52,53].

In the particular detergent-free core particles as used in this study, the detectable release of protons is slowed down due to diffusion/reaction of protons between aggregated particles [41]. In thylakoids, on the other hand, high rates of proton release have been resolved due to the collisional transfer between donor groups and the membrane-adsorbed indicator dye Neutral red [47]. Core particles containing detergent are monodisperse and showing very rapid proton release [17,45]. The latter material lacks the 17 and 23 kDa extrinsic proteins [72], which, in our hands, were present in the aggregated core particles prepared according to [40]. The monodisperse, polypeptide-depleted core particles prepared after [72] were less robust to Cl^- depletion, e.g., aging occurred more rapidly and they were therefore not used in this work. Aiming at higher time resolution of proton release, we used thylakoids. These were chloride-depleted (see Materials and Methods) and dark-adapted, and proton release was recorded by Neutral red as function of the flash number (Fig. 4A). At pH 7.4 in the control (top), a pronounced oscillation of the proton over electron stoichiometry was observed (the pattern was about 0.5:1:1.5:1 starting with flash No. 1, as reported previously [47]) at variance with the result in core particles, where the pattern was about 1:1:1:1 at any pH tested (compare Fig. 3A). Without chloride (Fig. 4A, bottom), proton release on the first flash was 2-fold greater than in controls. It declined to about 30% of the former figure from the third flash on. When this set of experiments was repeated at pH 6.1 (data not shown) we observed the release of about 1.5 protons on the first flash in controls as previously reported [47]. Without chloride this figure was reduced to only about one proton. These figures obtained in reversibly Cl^--depleted material differed from those which we previ-
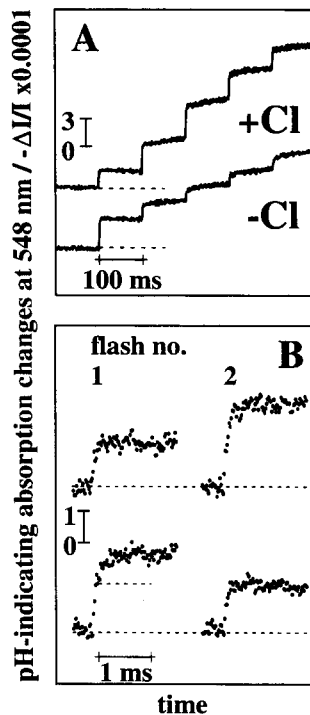
Fig. 4. (A) Proton release after the first five flashes in dark-adapted, unstacked Cl⁻-depleted (lower trace) and control (upper trace) thylakoids (30 μM chlorophyll) measured with Neutral red at 548 nm (30 μM, ±dye). The time resolution was 1 ms per address, 30 transients were averaged. (B) proton release on the first two flashes in unstacked thylakoids (+Cl⁻, top; −Cl⁻, bottom) measured with Neutral red (30 μM) plus imidazole (300 μM) at 548 nm (±dye). The first flash was measured with 30 μM DCMU to avoid transient contributions of proton uptake from the acceptor side [71]. Conditions: 30 μM of chlorophyll, 20 μs per address, up to 300 transients averaged. Excitation: first flash, ruby laser; subsequent flashes, xenon lamp.

ously reported for Cl⁻-depleted thylakoids [30]. In the cited study the reversibility of chloride depletion was less well controlled due to harsher preparation procedures and the proportion of double hits was larger (xenon flash instead of Q-switched ruby laser as in this work).

We time-resolved proton release on the first and second flash at pH 7.4 (Fig. 4B). In the controls (top) the release of 0.5 and 1 proton proceeded monophasically with an apparent half-rise-time of 60 μs. In Cl⁻-depleted material (bottom) the first flash induced the release of about 0.5 protons with 60 μs. The fast release was followed by a slower one (dotted line) of about equal magnitude with a half-rise-time of 220 μs. On the second flash, about 0.5 protons were released but now monophasically with a half-rise-time of again 60 μs. Thus, Cl⁻-depletion of thylakoids produced an additional slow component of proton release on the first flash.

3.6. Chloride depletion impairs the formation of the normal S_2 state

By monitoring in Cl⁻-depleted core particles UV absorption transients at 320 nm and local electrochromism at

443 nm we attempted to characterize further the components that were oxidized on the first two transitions. Fig. 5A shows UV transients at 320 nm induced by the first 5 out of 9 recorded flashes in dark-adapted Cl⁻-depleted material (bottom) and controls (top). The stable jumps were attributable to donor side events [46]. They were obtained as previously [46], by subtracting transients measured under repetitive excitation (1 Hz) and attributable to the acceptor side from transients obtained with dark-adapted material. In the control, the normal oscillations of the jumps were correctly described by the set of relative extinction coefficients attributable to transitions $S_i \Rightarrow S_{i+1}$ as given by Lavergne [13], namely -0.1, 1.1 and 0.5 (starting from S_0). With these figures and the following Kok parameters: (misses) $\alpha = 0.1$, (double hits) $\beta = 0$ and the relative proportion of centers initially in $S_0 = 20\%$ and in $S_1 = 80\%$, the expected behavior is given in Fig. 5A by triangles. The fair agreement indicated that Cl⁻-repleted centers were well synchronized in the dark. The deviation on the first flash was probably caused by centers that were damaged at the acceptor side [54] and capable of only one turnover. Without chloride (lower trace), the first flash induced a stable jump of only about 65% of the control and the transient on the second flash was smaller. From the third flash on only short-lived transients but no stable changes after 50 ms were detected.

A similar protocol was applied to record electrochromic transients at 443 nm (Fig. 5B). The major sources of electrochromic transients at this wavelength are charges on
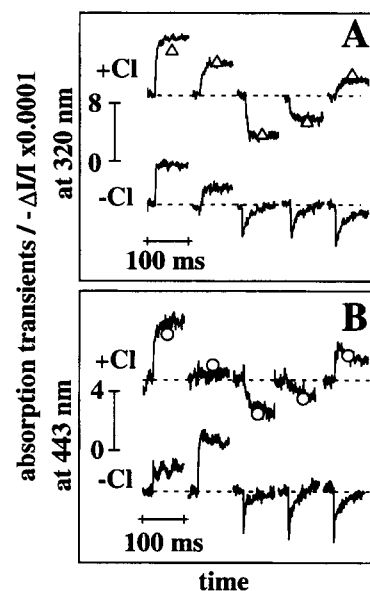

Fig. 5. Absorption transients induced by the first five out of nine recorded flashes in dark-adapted core particles (A) at 320 nm and (B) at 443 nm. Top: control; bottom, Cl⁻-depleted. The transients result from the differences between recordings with dark-adapted material with or without Cl⁻ and material under repetitive excitation with Cl⁻. The patterns of triangles and circles were calculated with the parameters in the text. Conditions: 1 ms per address, 30 transients averaged, 5 μM chlorophyll.

Mn and Y_Z [48,50]. With chloride (top) the quaternary oscillation of the jumps was readily described by relative extents of 0:1:0:− 1 as shown previously [17]. Open circles indicate the calculated oscillations under these conditions. Without chloride (bottom) this pattern was changed. The transient on the first flash was much smaller and the one on the second flash was larger than in the control. From the third flash on, no stable changes were detected. Again, it was evident that the electrostatic situation was severely altered by the absence of chloride already during the first transition.

3.7. Similar optical difference spectra are induced by the first flash in Cl⁻-depleted and the second flash in control centers

The extents of absorption transients at 50 ms after the first two flashes were measured in dark-adapted, Cl⁻-depleted core particles and in controls in a wavelength range from 290 to 450 and from 630 to 720 nm (see Materials and Methods). These transients were calibrated in terms of molar extinction $(\Delta\epsilon)$ using the antenna size of 120 chlorophylls per reaction center. They were plotted in Fig. 6. The spectra obtained on the respective first flash were corrected by 0.15 times the spectrum attributable to Q_A^- formation shown in Fig. 6F to account for the contribution of about 15% of centers on the first flash (compare Fig. 5A) which were fully inhibited at the acceptor side [54]. No further corrections, e.g., for fully active centers in Cl⁻-depleted material or for the miss factor, were applied. In controls, the first flash produced a difference spectrum similar to the one reported for S_2 formation (see for example [13]) (Fig. 6A). Its major component in the red spectral region was a blue electrochromic bandshift of one or several pigments. A detailed analysis of these band shifts has been described elsewhere [68]). The extents upon the second flash (Fig. 6B) were about 2-times smaller in the UV than the ones on the first flash as reported previously [13]. Stable local electrochromism as observed around 440 nm was negligible. In the red part of the spectrum only small electrochromic bandshifts were observed. In the region around 390 nm the shape of our spectrum on the second flash differed considerably from the spectrum reported for transition $S_2 \Rightarrow S_3$ by Lavergne [13] and to lesser extent also from the one of Van Leeuwen et al. [14] (the latter two spectra were plotted in Fig. 6B as dashed and dash-dotted lines for comparison, normalized at 310 nm). The $S_2 \Rightarrow S_3$ spectrum reported by Dekker et al. [15] differed even more strongly from all these spectra. These differences are still poorly understood.

In Cl⁻-depleted material the first flash (Fig. 6C) induced a difference spectrum resembling the one observed on the second flash in the controls. In the UV, the amplitudes were somewhat larger than in the latter spectrum but smaller than on the normal $S_1 \Rightarrow S_2$ transition. Stable electrochromism in the blue as well as in the red part of
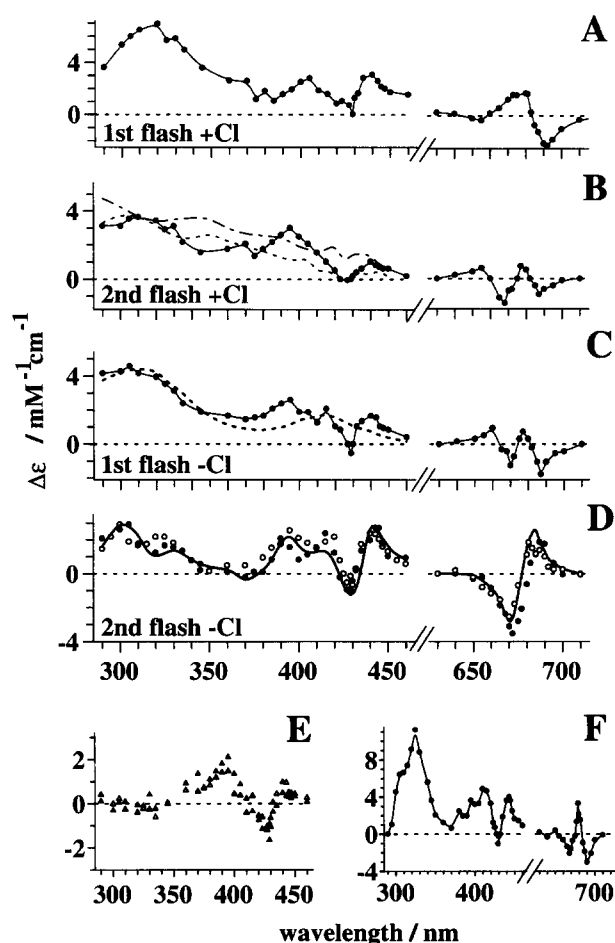

Fig. 6. Flash-induced optical difference spectra of core particles. (A) and (B) Control, 1st and 2nd flash; (C) and (D): Cl⁻-depleted, 1st and 2nd flash. The dashed and dash-dotted lines in (B) represent the spectra attributed to $S_2 \Rightarrow S_3$ in [13] and [14], the dashed line in C is the His'-OH/His spectrum from [73]. For the symbols in D see text. (E) Solid triangles, difference (2nd flash +Cl⁻) minus (His'-OH/His); open triangles, difference (1st flash −Cl⁻) minus (His'-OH/His). (F) Spectrum of Q_A^-/Q_A obtained under repetitive flash excitation. For details see text. Note different scaling factors on the Y-axes.

the spectrum was also much smaller than in the normal $S_1 \Rightarrow S_2$ transition and again similar to the one of the normal $S_2 \Rightarrow S_3$ transition. Around 350 nm the relative magnitude compared to the one at 310 nm was smaller than in the spectra attributed to $S_2 \Rightarrow S_3$ by other authors [13,14]. Our spectrum more closely resembled the one obtained on the first flash in Ca^{2+}-depleted centers that has been attributed to histidine oxidation [31]. The second flash (Fig. 6D) induced only small changes in the UV, but large electrochromism in the blue and red part of the spectrum. This spectrum (closed circles) was very similar in the UV and blue region to the one attributed to Y_Z^{ox} in Tris-washed material [50,55]. The $Y_Z^{red} \rightarrow Y_Z^{ox}$ spectrum from [55] was also plotted in Fig. 6D (blue part) for comparison (thick smooth line, normalized by a factor of 0.8). In the red a pronounced electrochromic red shift was observed. Such a band shift has been reported before and

attributed to Y_Z^{ox} (Dekker, J.P. (1985) PhD Thesis, University of Leiden). A spectrum similar to the one of $Y_Z^{red} \rightarrow Y_Z^{ox}$ was also obtained under repetitive excitation (period of 5 s) with Cl^--depleted centers (not shown) or Tris-washed material (Fig. 6D, open circles, data points normalized by a factor of 0.75). In the latter two measurements, the extents were about 1.25-times larger than on the second flash without chloride. From these results we conclude that the second flash produces Y_Z^{ox} in about 70–80% of Cl^--depleted centers.

An in vitro difference spectrum of the oxidized, neutral OH adduct of histidine has been reported in [73]. It was plotted (broken line) in Fig. 6C ($\times 0.75$) for comparison. We subtracted it from the spectra in Fig. 6B and C (normalized for equal extents at 320 nm). The results are shown in Fig. 6E (Fig. 6B minus His, closed triangles; Fig. 6C minus His, open triangles). Both differences mainly exposed a small and broad electrochromic blue shift around 410 nm. In the UV the differences were negligible. This was compatible with the notion that the oxidized component after the first flash given to Cl^--depleted and dark-adapted core particles was histidine.

3.8. The kinetics of electron transfer to Y_Z^{ox}

The oxidation/reduction of the known (Mn, Y_Z) and hypothetical (His) redox cofactors of the OEC is accompanied by absorption changes in the UV. We monitored the oxidation of the OEC by Y_Z^{ox} at 295 nm as induced by the first two flashes. The absorption transients at 295 nm are not directly and solely attributable to the reduction of Y_Z^{ox} itself, but rather indirectly through a superimposition of absorption transients resulting from the oxido/reduction of Y_Z^{ox} plus the oxidation of the manganese/histidine cluster. Still their time course follows the reduction of Y_Z^{ox}. Original graphs are shown in Fig. 7A. In controls (top) the first flash caused an unresolved jump, mainly attributable to the formation of Y_Z^{ox} by P_{680}^+ (see Fig. 6D, F) in less than 1 μs. Its level is indicated by a broken line. It followed a slower rise attributable to the oxidation of the OEC by Y_Z^{ox} with a half-rise-time of 80 μs. On the second flash the jump was followed by a rise with a half-rise-time of 240 μs and of smaller extent as on the first flash. These two half-rise-times are typical for Y_Z^{ox} reduction by the OEC during transitions $S_1 \Rightarrow S_2$ and $S_2 \Rightarrow S_3$ in controls (see Introduction). In Cl^--depleted material (bottom) the first flash induced the same fast jump. Again it was followed by a slow rise but with longer half-rise-time of 220 μs. On the second flash there was no slow rise, in contrast to the control. The jump indicated the stable formation of Y_Z^{ox}.

The same set of experiments was carried out in the blue region of the spectrum where local electrochromism is observed (see above). First we measured the transients at 443 nm. These transients are a superimposition of components from the acceptor and the donor side. The acceptor side components were measured separately under the same
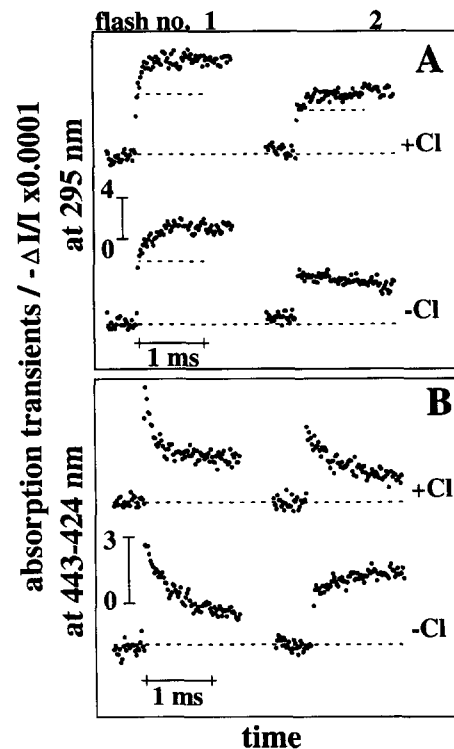

Fig. 7. Time resolution of electron transfer in controls (top) and Cl^--depleted (bottom), dark-adapted PSII core particles as induced by the first two flashes. (A) Transients at 295 nm and (B) at 443–424 nm obtained with core particles. Conditions: 5 μM of chlorophyll, 20 μs per address, up to 200 transients averaged. Excitation: 1st flash, ruby laser; subsequent flashes, xenon lamp.

conditions at 424 nm [18] and subtracted. The resulting transients which are documented in Fig. 7B are attributable to donor side events [18]. In the controls (top) the extent of the rapid jump induced by the first flash can be attributed to electrochromism caused by Y_Z^{ox} formation in nanoseconds. The jump was followed by a decay due to the reduction of Y_Z^{ox} by the OEC to a stable level above the baseline with a half-decay time of 100 μs. On the second flash a slower decay to the baseline with a half-decay time of 260 μs was observed. The decay-times of the electrochromic transients were similar to the rise-times observed at 295 nm which indicated that they were due to the same event, namely to the forward electron transfer to Y_Z^{ox}. The minor deviations may be caused by the procedure of taking differences of recordings at two wavelengths (see also Rappaport et al. [18]). The microsecond components of P_{680}^+ reduction [56] contribute to both wavelengths, 443 and 424 nm (see for example [57]). Thus, a small portion of the electrochromic signal of the higher S-states may be cancelled out by these contributions.

In the absence of chloride (bottom) the jump on the first flash was followed by a slower decay, half-decay time 270 μs, to a stable level that was smaller than in the control (see also Fig. 5). On the second flash the jump was not followed by a decay but by a small and slower rise to a

Table 2

Half-rise-times of electron transfer to Y_Z^{ox} in Cl^--depleted core particles $(-Cl^-)$ and controls $(+Cl^-)$ based on UV transients and local electrochromism as derived from documents in Fig. 7A, B

Flash number:		1	2
Observable:	Cl^-:	half-rise-time (μs)	
UV-transients (295 nm)	+	80	240
	–	220	(ms)
Local electrochronism (443–424 nm)	+	100	260
	–	270	(ms)
Proton release (548 nm)	+	60 (0.5)	60 (1.0)
	–	60 (0.5)	60 (0.5)
		210 (0.5)	

Data on proton release in Cl^--depleted thylakoids and controls derived from Fig. 4C. (ms) denotes the slow decay of Y_Z^{ox}. The relative extents of proton release are given in parentheses. For details see figures and text

level which was stable in the measuring interval. The latter rise was probably again due to a small superimposed transient resulting from the reduction of P_{680}^+. The half-rise-times of electron transfer as derived from electrochromism and UV transients are summarized in Table 2 and compared with those of proton release in thylakoids (see Section 3.5). We conclude that the first two flashes of light produced mainly states S_2 and S_3 in controls. The half-rise-times were 80 and 250 μs, respectively. In Cl^--depleted centers another component was oxidized on the first flash with a similar half-rise-time as found during transition $S_2 \Rightarrow S_3$ in controls, namely 240 μs. This half-rise-time approximately matched the one of the slow additional proton release on the first flash (compare Fig. 4B) in Cl^--depleted thylakoids.

4. Discussion

Driven by four quanta of light which oxidize the primary electron donor, P_{680}, the oxygen evolving complex accumulates four oxidizing equivalents to finally liberate oxygen from water. We compared the storage of oxidizing equivalents in Cl^--depleted and control Photosystem II. The OEC was stepped forward by a series of light flashes given to dark adapted samples, and electron and proton transfer were kinetically resolved by flash-spectrophotometry in the visible, near UV and IR. The prevalence in the dark of the same oxidation state, namely S_1 of the OEC in reversibly Cl^--depleted material as in controls is inferred from the literature. It has been established that the addition of Cl^- after exposure of dark-adapted Cl^--depleted material to a single flash of light restored the EPR multiline signal that characterizes the second oxidation state, S_2 [28].

We found that only two oxidizing equivalents are to be stored on the OEC in reversibly Cl^--depleted material, in line with the literature [28,29]. A third flash produced P_{680}^+

which rapidly (in about 150 μs) backreacted with Q_A^-. After the first two flashes of light, P_{680}^+ was reduced in nanoseconds. This behavior was independent of the presence or absence of chloride, as if reversible Cl^- depletion did not affect the coupling between Y_Z and P_{680}^+. This result differed from the one observed with Mn-depleted ([42], and this work) and calcium-depleted [29] centers. In these materials the reduction of P_{680}^+ is slowed down from nano- to microseconds.

Y_Z was probably the secondary electron donor both in Cl^--depleted material and in controls. In controls the half-life times of the Y_Z radical are about 100 and 240 μs after the first two flashes of light ([16,18] and this work). In Cl^--depleted material we found about 250 μs for the first and about 450 ms for the second flash. During these intervals the Y_Z radical was the (meta-)stable product also in Cl^--depleted material. The more stable formation of the Y_Z radical on the second transition has previously been reported based on EPR studies on Cl^--free BBY membranes [35]. Both lines of evidence are inconsistent with the proposal that manganese is oxidized on the second flash [36]. The proposal that Mn is oxidized [36] has been based mainly on a broad EPR signal (16 mT) at $g = 2$ which has been observed on the second transition both in Cl^--free [36,37] and in calcium-free material [32,58,59]. It has been tentatively attributed to oxidized histidine in magnetic interaction with manganese [36]. Our results on chloride-depleted centers imply instead that this signal is caused by the Y_Z radical as proposed before for calcium-depleted centers [60]. Whether the modification of the line shape of the Y_Z radical is directly attributable to its magnetic interaction with the X radical, the product formed after the first flash, or to a changed protonation state of the Y_Z environment (see further down) remains to be established.

After the first flash given to dark-adapted samples, X^{ox} appeared in about 240 μs. This half-rise-time was similar to the one during transition $S_2 \Rightarrow S_3$ in the control. The difference spectrum of $X^{red} \rightarrow X^{ox}$ (the first transition in Cl^--depleted material) resembled the one induced by the second flash (transition $S_2 \Rightarrow S_3$) in controls. Both spectra resembled the difference spectrum of the chemical oxidation of histidine to its OH^- adduct in vitro [31,73], except for slightly different and small electrochromic components in the blue and red spectral regions. X stayed oxidized for at least 5 s (this figure is only the lower limit under our measuring conditions). According to Ono et al. [28], the component formed on the first flash without Cl^- is even more stable, for about 5 min. In unperturbed material, state S_3 has been reported to decay in about 4 min [61]. The kinetic and spectral evidence supports the notion that the same component, X, is oxidized on the first transition without chloride and on the second one, namely $S_2 \Rightarrow S_3$, in controls. X may be histidine.

Accordingly, we propose the following sequence of events. In controls, the first two steps are $S_1 \Rightarrow S_2 \Rightarrow S_3$.

We interpret this sequence as $\check{S}_1 XY_Z \Rightarrow \check{S}_2 XY_Z \Rightarrow \check{S}_2 X^{ox} Y_Z$. By $\check{S}_1$ and $\check{S}_2$ we denote the first and second oxidized state of {Mn$_4$ plus bound water} itself. Accordingly, in chloride-depleted centers the first two steps are as follows: $\check{S}_1 XY_Z \Rightarrow \check{S}_1 X^{ox} Y_Z \Rightarrow \check{S}_1 X^{ox} Y_Z^{ox}$.

The deposition of a positive charge on either Mn and Y_Z induces a transient electrochromic response of the innermost pigments of PS II (Chl a and Pheo a) (see [18] and this work). We have recently shown that proton release in PS II core particles and thylakoids is largely a peripheral electrostatic phenomenon [17,47,64] which affects neither the rates nor the extents of these local electrochromic responses [17]. Transition $S_1 \Rightarrow S_2$ in controls causes rapid (10 μs) proton release from amino acids in the vicinity of Y_Z^{ox} which persists upon its reduction by the Mn cluster [45,47]. According to EPR studies, Y_Z^{ox} is a neutral radical [5]. Electroneutrality requires that the oxidation of Y_Z displaces one hydroxyl proton from its phenol ring to a neighboring proton acceptor, a proton rocking motion similarly as described for the oxidation of its counterpart Y_D [62,63]. Although Y_Z^{ox} is electroneutral, its big electrochromic effect clearly shows that the positive charge (e.g., the proton) resides in its close vicinity. The *observable* fast proton release *into the medium* is a different event. Its relative extent, kinetically at the level of Y_Z^{ox}, is highly variable on the first transition. It ranges from 0.5 to 1.5 depending on the pH in control thylakoids ([47], and this work), it is 0.5 in Cl$^-$-depleted thylakoids at pH 7.4 (this work) and always about one in core particles ([41,45,46] and this work). In all cases the formation of Y_Z^{ox} causes a large electrochromic transient in controls and a large stable jump in reversibly Cl$^-$-depleted or Mn-depleted material (compare Fig. 6D and Fig. 7B). In contrast to the variable extent of proton release caused by the first flash of light (mainly $S_1 \Rightarrow S_2$ in controls), the second flash (transition $S_2 \Rightarrow S_3$ again in controls) causes the release of 1 proton in different types of material and at any pH studied (reviewed in [64]). The peripheral protolytic reactions did not compensate the positive charge in the vicinity of Y_Z^{ox} or the one on Mn in S_2. In contrast with this behavior of Y_Z^{ox}, the formation of X^{ox} (e.g., after the first transition in Cl$^-$-depleted samples) caused only small electrochromic band shifts. The same holds true for transition $S_2 \Rightarrow S_3$ in controls. This is again compatible with the notion that the same component, X, is oxidized during these two transitions.

There are several possible causes for the small magnitude of electrochromism. The positive charge on X may be compensated by releasing a proton from X *into the medium*. Alternatively, it is conceivable that a charged radical is formed, X^+, but being unfavorably placed relative to the electrochromically active pigments. Two lines of evidence are in favor of a direct chemical deprotonation of X^{ox} as contrasting with a peripheral electrostatic response (for further evidence see Appendix). (i) Transition $S_2 \Rightarrow S_3$ in control material releases one proton per electron into the
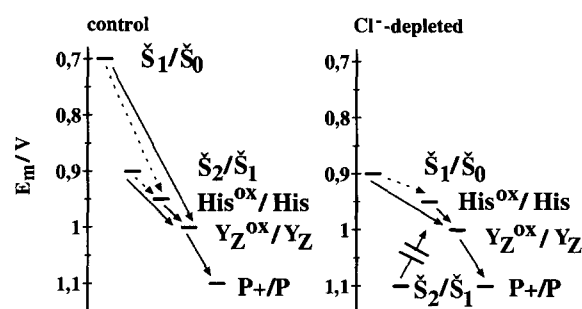
Scheme 1. Midpoint potentials and suggested pathways of electron transfer at the electropositive side of PS II in control and Cl$^-$-depleted Photosystem II. Control: The hypothetical intermediate oxidation of His during transitions $S_0 \Rightarrow S_1$ and $S_2 \Rightarrow S_3$ (see text) is indicated by broken arrows. Cl$^-$-depleted: altered midpoint potentials of the Mn redox couples $\check{S}_1/\check{S}_0$ and $\check{S}_2/\check{S}_1$. Transition $S_1 \Rightarrow S_2$ is inhibited, whereas $S_0 \Rightarrow S_1$ still functions. For references on the respective midpoint potentials see text.

medium in all oxygen evolving materials and at any pH (for review see [64]). The same holds true for the first transition in Cl$^-$-depleted samples. (ii) In Cl$^-$-depleted thylakoids (pH 7.4) the first flash of light causes the rapid release of less than one proton (electrostatically driven) followed by the additional slow release of about 0.5 proton. Its half-rise-time matched that of the formation of X^{ox}. Chloride depletion may thus expose the slower chemical deprotonation of X^{ox} that, in controls, is kinetically masked by the transient, fast, and electrostatically triggered proton release by $(Y_Z^{ox} + H_{displaced}^+)$ on transition $S_2 \Rightarrow S_3$ [47].

We propose a simple electrostatic role of Cl$^-$ in the OEC. Earlier EXAFS studies have been interpreted to exclude Cl$^-$ from the first coordination shell of manganese [11], in more recent ones from the same laboratory this view has been revised [76]. We propose that Cl$^-$ functions to modulate the midpoint potential of the manganese cluster as illustrated in Scheme 1: In the presence of chloride (and calcium) the midpoint potential of the redox couple S_2/S_1 is about +900 mV [67]. By removal of chloride this potential may increase by 100–300 mV to, say, +1.1 V. Let us assume that the component X is histidine. The midpoint potential of His has been reported to be about +0.95 V ([31] and references therein) and the potential of Y_Z to about +1 V [69]. If Cl$^-$ depletion raised the potential of S_2/S_1 above +1 V, the manganese cluster was no more to be oxidized and electron transfer stopped at Y_Z or His. In the absence of chloride, we observed that His^{ox} was formed on the first and Y_Z^{ox} on the second transition. If the readdition of chloride lowered the potential difference between S_2 and S_1, the oxidation by His^{ox} of the Mn-cluster became possible and it resulted in the formation of the multiline S_2 state in the dark as reported in the literature [70]. If Cl$^-$ depletion raised the midpoint potential of the couple S_1/S_0 by a similar figure from about +700 mV [67] to +900 mV, it would still be lower

than the ones of both His and Y_Z. Thus, Y_Z could still oxidize Mn and transition $S_0 \Rightarrow S_1$ still functioned (although probably with altered kinetics). This explained the presence of mainly S_1 in the dark, as experimentally observed.

Is X^{ox} (His^{ox}) only produced (by Y_Z) during $S_2 \Rightarrow S_3$ in normal material where it remains stable for about 4 min, or transiently also during the other transitions? It is still conceivable that the cofactors Mn-X-Y_Z-P_{680} are arranged in a sequential reaction scheme (indicated by the broken arrows in Scheme 1), with the electron transfer reaction $X \rightarrow Y_Z^{ox}$ rate limiting (rise-times of 30 and 60 μs) and reaction $Mn \rightarrow X^{ox}$ during transitions $S_0 \Rightarrow S_1$ and $S_1 \Rightarrow S_2$ faster (say at 1 μs). Then X^{ox} is not accumulated to any appreciable extent. The sequential arrangement of Mn, X, Y_Z and P_{680} places X closer to Mn than Y_Z. That the EPR S_2 state multiline signal can be simulated under the assumption of histidine ligation to Mn [74] supports the above notion. The oxidation of His in S_3 further implies that transition $S_3 \Rightarrow S_4$ is truly $\check{S}_2 X^{ox} Y_Z \Rightarrow \check{S}_2 X^{ox} Y_Z^{ox}$. This implies that, of the four oxidizing equivalents, only two are stored on Mn itself. The last charge, which is stored as ($Y_Z^{ox} + H^+_{displaced}$), electrostatically ignites the final step of oxygen production. Model studies with synthetic Mn compounds have led to the proposal of a mechanism which involves the destabilisation of a μ-oxo-bridge of the Mn cluster by a proton from oxidized histidine in state S_3 [9]. The chemical deprotonation of X^{ox} *into the medium* and also the recent observation that only one of the two substrate water molecules is tightly bound in S_3 [75] argue against this suggestion. Alternatively, it can be considered that the neutral His radical accepts an electron plus a proton on transition $S_4 \rightarrow S_0$, such that the energy barrier of the final step of water oxidation and oxygen release is lowered by concomitant electron and proton, i.e., hydrogen transfer [7].

5. Conclusions

In Cl^--depleted and dark-adapted reaction centers the first flash of light oxidizes a component X. According to its UV difference spectrum X may be histidine. In control material, the same component is oxidized only after the second flash, inducing transition $S_2 \Rightarrow S_3$. The most likely interpretation of our data on local electrochromism, P_{680}^+ reduction, electron transfer and proton release is that X deposits one proton into the medium after its oxidation by Y_Z^{ox}. After the first two flashes of light given to dark-adapted and Cl^--depleted samples Y_Z functions as the nanosecond electron donor to P_{680}^+. The effects of chloride depletion are straightforwardly explained by the assumption that the absence of this anion increases the midpoint potential of the manganese redox couples S_1/S_0 and S_2/S_1 by about 300 mV to more than 1.1 V. This inhibits the oxidation of manganese by Y_Z and thereby transition

$S_1 \Rightarrow S_2$. $S_0 \Rightarrow S_1$, on the other hand, may still function. When Y_Z^{ox} is formed during transition $S_3 \Rightarrow S_4$ it ignites the final step of water oxidation wherein the oxidized and deprotonated component X^{ox} accepts a proton plus an electron.

Appendix A

A.1. On the reduction of P_{680}^+ in nanoseconds and its relation to protolytic events

In dark-adapted samples, the rate of reduction of P_{680}^+ oscillates with period of four as function of the flash number. On transitions $S_2 \Rightarrow S_3$ and $S_3 \Rightarrow S_4$ the reduction is biphasic (see [65] and this work). The oscillation has been explained as reflecting the storage of uncompensated charges in the OEC [22]. The biphasicity has originally been attributed to two serial donors to P_{680}^+ [19]. Integrating our data on P_{680}^+ reduction and proton release in Cl^--depleted and control material we arrived at an alternative explanation for the biphasicity that is better compatible with further data.

In control material ($+ Cl^-$), the reduction of P_{680}^+ is fast and monophasic on the first but slower and biphasic on the second transition. Without chloride it is monophasic on both transitions, but again slower on the second than on the first one. We interpret these variations in terms of the electrostatic effect of acid/base groups in closer proximity to Y_Z than to P_{680}. Deprotonation of an acid at the membrane/water interface or within the membrane creates a negative directed jump of the electrostatic potential, here in the vicinity of Y_Z. This accelerates the electron transfer to P_{680}^+. The exchange of protons on surface exposed groups with a pK equal to the given pH (here 6.5) is rather slow. The upper limit of the rates is reached if the on-reaction is diffusion controlled ($k_{on} \cong 10^{11}$ s^{-1}). The off-rate constant is related to the pK according to $k_{off} = K \cdot k_{on}$ with $K = 10^{-pK}$. If pH = pK = 6.5, the off rate amounts to $10^{-6.5} \cdot 10^{11}$ s$^{-1} \sim 3 \cdot 10^4$ s^{-1}. The expected relaxation time is about 30 μs at pH 6.5. Under these conditions such a group is half protonated both as the ensemble average over several reaction centers and as the time average for a given reaction center over time intervals much longer than

the relaxation time. In the nanosecond time-scale, however, the group is deprotonated in one half of the set of reaction centers and protonated in its complement. This heterogenicity at the nanosecond time scale may be responsible for the seemingly biphasic reduction of P_{680}^+. The slowing of P_{680}^+ reduction in controls [65] and in Tris-washed material [42] at acidic pH is compatible with this concept. We interpret the monophasic reduction of P_{680}^+ on the first transition as indicating the full protonation of the relevant groups independent of the absence or presence of chloride. In controls, the first flash creates state $\check{S}_2$ (we denote by $\check{S}_2$ the second oxidized state of Mn itself) that (according to the above cited data on local electrochromism) carries one positive extra charge on the manganese cluster. In addition, there is proton release from peripheral groups. These groups are heterogeneously protonated (some AH and some A^-) on the nanosecond timescale. During *the next* electron transfer step the heterogeneity becomes apparent. In reaction centers with protonated groups the rate of electron transfer is slowed down by a factor of about 20 (from 15 to 280 ns) due to the charge on manganese ($\check{S}_2$) plus the superimposed effect of the protonated acid/base groups. In centers with deprotonated groups their effect counteracts the deceleration by the charge on manganese and decreases the factor to about 2.5 (15 to 40 ns).

The oxidized component, X^{ox}, which is formed on the second step slows *the third* electron transfer step much less than the charge on $\check{S}_2$, namely by a factor of only about 1.5 (controls, from 40/280 ns to. 60/390 ns). The same holds true for chloride-depleted centers where X^{ox} is formed on the first flash. Here the rate on *the second* flash is slowed only by a factor of about 3 (Cl^--depleted, from 35 to 100 ns). The biphasicity in controls; and the monophasicity in Cl^--depleted centers, on the other hand, were unchanged. This behavior was readily understood if the initial protonation state of the acid/base groups (heterogenous in controls; homogenous in Cl^--depleted centers) was not changed by the formation of X^{ox}. This can be understood by the rebinding of the electrostatically released protons (upon formation of Y_Z^{ox}) concomitant with the release of a proton from X^{ox} itself. The minor deceleration of electron transfer in the presence of X^{ox} may indicate a structural change on transition $S_2 \Rightarrow S_3$ as proposed earlier [66]. The conclusion that Y_Z does not release a "chemical proton" whereas X does may indicate that hydrogen bond acceptors are lacking around X. This places X in a more hydrophobic environment than Y_Z.

References

[1] Wyrdrzynski, T. (1993) Oxygen Evolution in Photosynthesis. In Photosynthesis: Energy Conversion by Plants and Bacteria, Cell Biology (Govindjee, ed.), pp. 469–495, Academic Press, London.

[2] Renger, G. (1992) Energy Transfer and Trapping in Photosystem II. In The Photosystems: Structure, Function and Molecular Biology (Barber, J., ed.), pp. 45–99, Elsevier, Amsterdam.

[3] Rutherford, A.W., Zimmermann, J.L. and Boussac, A. (1992) Oxygen Evolution. in The Photosystems: Structure, Function and Molecular Biology (Barber, J. ed.), pp. 179–229, Elsevier, Amsterdam.

[4] Renger, G. (1987) Photosynthetica 21, 203–224.

[5] Babcock, G.T., Barry, B.A., Debus, R.J., Hoganson, C.W., Atamian, M., McIntosh, L., Sithole, I. and Yocum, C.F. (1989) Biochemistry 28(25), 9557–9565.

[6] Witt, H.T. (1991) Photosynth. Res. 29, 55–77.

[7] Krishtalik, L.I. (1990) Bioelectrochem. Bioenerg. 23, 249–263.

[8] Padhye, S., Kambara, T., Hendrickson, D.N. and Govindjee (1986) Photosynth. Res. 9, 103–112.

[9] Pecoraro, V.L. (1992) in Manganese Redox Enzymes (Pecoraro, V.L., ed.), pp. 197–231, VCH, New York.

[10] Dismukes, G.C. and Siderer, Y. (1981) Proc. Natl. Acad. Sci. USA 78, 274–278.

[11] Sauer, K., Yachandra, W.K., Britt, R.D. and Klein, M.P. (1992) in Manganese Redox Enzymes (Pecoraro, V.L., ed.), pp. 141–175, VCH, New York.

[12] Ono, T., Nogushi, T., Inoue, Y., Kusunoki, M., Matsushita, T. and Oyanagi, H. (1992) Science 258, 1335–1337.

[13] Lavergne, J. (1991) Biochim. Biophys. Acta 1060, 175–188.

[14] Van Leeuwen, P.J., Heimann, C. and Van Gorkom, H.J. (1993) Photosynth. Res. 38, 323–330.

[15] Dekker, J.P., Van Gorkom, H.J., Wensink, J. and Ouwehand, L. (1984) Biochim. Biophys. Acta 767, 1–9.

[16] Dekker, J.P., Plijter, J.J., Ouwenand, L. and Van Gorkom, H.J. (1984) Biochim. Biophys. Acta 767, 176–179.

[17] Haumann, M., Bögershausen, O. and Junge, W. (1994) FEBS Lett. 355, 101–105.

[18] Rappaport, F., Blanchard-Desce, M. and Lavergne, J. (1994) Biochim. Biophys. Acta 1184, 178–192.

[19] Brettel, K., Schlodder, E. and Witt, H.T. (1984) Biochim. Biophys. Acta 766, 403–415.

[20] Saygin, Ö. and Witt, H.T. (1985) Photobiochem. Photobiophys. 10, 71–82.

[21] Rappaport, F. and Lavergne, J. (1991) Biochemistry 30, 10004–10012.

[22] Witt, H.T., Schlodder, E., Brettel, K. and Saygin, Ö. (1986) Photosynth. Res. 10, 453–471.

[23] Haumann, M. and Junge, W. (1995) in Advances in Photosynthesis: Oxygenic Photosynthesis – The Light Reactions (Ort, D. and Yocum, C.F., eds.), in press, Kluwer, Dordrecht.

[24] Förster, V. and Junge, W. (1985) Photochem. Photobiol. 41, 183–190.

[25] Debus, R.J. (1992) Biochim. Biophys. Acta 1102, 269–352.

[26] Yocum, C.F. (1992) in Manganese Redox Enzymes (Pecoraro, V.L., ed.), pp. 71–83, VCH, New York.

[27] Theg, S.M., Jursinic, P.A. and Homann, P.H. (1984) Biochim. Biophys. Acta 766, 636–646.

[28] Ono, T., Conjeaud, H., Gleiter, H., Inoue, Y. and Mathis, P. (1986) FEBS Lett. 203, 215–219.

[29] Boussac, A., Setif, P. and Rutherford, A.W. (1992) Biochemistry 31, 1224–1234.

[30] Lübbers, K., Drevenstedt, W. and Junge, W. (1993) FEBS Lett. 336, 304–308.

[31] Boussac, A., Zimmermann, J.L., Rutherford, A.W. and Lavergne, J. (1990) Nature (London) 347, 303–306.

[32] Tso, J., Sivaraja, M., Philo, J.S. and Dismukes, C.G. (1991) Biochemistry 30(19), 4740–4747.

[33] Allakhverdiev, S.I., Klimov, V.V. and Demeter, S. (1992) FEBS Lett. 297, 51–54.

[34] Damoder, R., Klimov, V.V. and Dismukes, G.C. (1986) Biochim. Biophys. Acta 848, 378–391.

[35] Deak, Z., Vass, I. and Styring, S. (1994) Biochim. Biophys. Acta 1185, 65–74.

[36] Boussac, A. and Rutherford, A.W. (1994) J. Biol. Chem. 269, 12462–12467.

[37] Baumgarten, M., Philo, J.S. and Dismukes, G.C. (1990) Biochemistry 29, 10814–10822.

[38] Barry, B.A. (1993) Photochem. Photobiol. 57, 179–188.

[39] Rutherford, A.W. and Boussac, A. (1992) in Research in photosynthesis (Murata, N. ed.), pp. 21–27, Kluwer Academic, Dordrecht.

[40] Ghanotakis, D.F., Demetriou, D.M. and Yocum, C.F. (1987) Biochim. Biophys. Acta 891, 15–21.

[41] Lübbers, K. and Junge, W. (1990) in Current Research in Photosynthesis, Vol. I (Baltscheffsky, M. ed.), pp. 877–880, Kluwer, Dordrecht.

[42] Conjeaud, H. and Mathis, P. (1980) Biochim. Biophys. Acta 590, 353–359.

[43] Jahns, P., Lavergne, J., Rappaport, F. and Junge, W. (1991) Biochim. Biophys. Acta 1057, 313–319.

[44] Junge, W. (1976) in Chemistry and Biochemistry of Plant Pigments (Goodwin, T.W. ed.), pp. 233–333, Academic Press, New York.

[45] Bögershausen, O. and Junge, W. (1995) Biochim. Biophys. Acta 1230, 177–185.

[46] Lübbers, K., Haumann, M. and Junge, W. (1993) Biochim. Biophys. Acta 1183, 210–214.

[47] Haumann, M. and Junge, W. (1994) Biochemistry 33, 864–872.

[48] Lavergne, J. (1984) FEBS Lett. 173, 9–14.

[49] Mathis, P. and Setif, P. (1981) Isr. J. Chem. 21, 316–320.

[50] Dekker, J.P., van Gorkom, H.J., Brok, M. and Ouwehand, L. (1984) Biochim. Biophys. Acta 764, 301–309.

[51] Yerkes, C.T., Babcock, G.T. and Crofts, A.R. (1983) FEBS Lett. 158(2), 359–364.

[52] Renger, G. and Völker, M. (1982) FEBS Lett. 149, 203–207.

[53] Förster, V. and Junge, W. (1984) in Advances in Photosynthetic Research (Sybesma, C. ed.), pp. 305–310, Martinus Nijhoff/Dr W. Junk, The Hague.

[54] Lavergne, J. and Leci, E. (1993) Photosynth. Res. 35, 323–343.

[55] Schatz, G.H. and Van Gorkom, H.J. (1985) Biochim. Biophys. Acta 810, 283–294.

[56] Schlodder, E., Brettel, K. and Witt, H.T. (1985) Biochim. Biophys. Acta 808, 123–131.

[57] Gerken, S., Dekker, J.P., Schlodder, E. and Witt, H.T. (1989) Biochim. Biophys. Acta 977, 52–61.

[58] Boussac, A., Zimmermann, J.L. and Rutherford, A.W. (1989) Biochemistry 28, 8984–8989.

[59] Sivaraja, M., Tso, J. and Dismukes, G.C. (1989) Biochemistry 28, 9459–9464.

[60] Hallahan, B.J., Nugent, J.H.A., Warden, J.T. and Evans, M.C.W. (1992) Biochemistry 31, 4562–4573.

[61] Styring, S. and Rutherford, A.W. (1987) Biochemistry 26, 2401–2405.

[62] Rodriguez, I.D., Chandrashekar, T.K. and Babcock, G.T. (1987) in Progress in Photosynthesis Research (Biggins, J. ed.), pp. 471–475, Martinus Nijhoff, Dordrecht.

[63] Mino, H., Satoh, J., Kawamori, A., Toriyama, K. and Zimmermann, J.L. (1993) Biochim. Biophys. Acta 1144, 426–433.

[64] Lavergne, J. and Junge, W. (1993) Photosynthesis Research 38, 279–296.

[65] Meyer, B., Schlodder, E., Dekker, J.P. and Witt, H.T. (1989) Biochim. Biophys. Acta 974, 36–43.

[66] Renger, G. and Hanssum, B. (1992) FEBS Lett. 299, 28–32.

[67] Vass, I. and Styring, S. (1991) Biochemistry 30, 830–839.

[68] Mulkidjanian, A., Cherepanov, D., Haumann, M. and Junge, W. (1996) Biochemistry, in press.

[69] Metz, J.G., Nixon, P.J., Rögner, M., Brudvig, G.W. and Diner, B.A. (1989) Biochemistry 28, 6960–6969.

[70] Ono, T., Zimmermann, J.L., Inoue, Y. and Rutherford, A.W. (1987) in Progress in Photosynthesis Research (Biggins, J., ed.), pp. 653–656, Martinus Nijhoff, Dordrecht.

[71] Haumann, M. and Junge, W. (1994) FEBS Lett. 347, 45–50.

[72] Van Leeuwen, P.J., Nieveen, M.C., Van de Meent, E.J., Dekker, J.P. and Van Gorkom, H.J. (1991) Photosynth. Res. 28, 149–153.

[73] Rao, P.S., Simic, M. and Hayon, E. (1975) J. Phys. Chem. 79, 1260–1263.

[74] Ahrling, K.A. and Pace, R.J. (1995) Biophys. J. 68, 2081–2090.

[75] Messinger, J., Badger, M. and Wydrzynski, T. (1995) Proc. Natl. Acad. Sci. USA 92, 3209–3213.

[76] Klein, M.P., Sauer, K. and Yachandra, V.K. (1993) Photosynth. Res. 38, 265–277.